# Finite Element Analysis and Strengthening of Bahr-Mowees Masonry Regulator

**Tarek El-Salakawy[1], Gehan Hamdy[1] , Mohie-Eldien Mohamed[2], Reem Elwan**

*[1] Civil Engineering Department, Faculty of Engineering at Shoubra, Benha University, Egypt*
*[2] Construction Research Institute, National Water Research Center, Egypt*
**corresponding author: tarik.abdelgalil@feng.bu.edu.eg*

## Abstract

The paper presents modeling and structural analysis for a 132-year-old masonry head regulator constructed on an irrigation canal in Egypt. Finite element modeling using nonlinear material properties are performed using finite element analysis program ANSYS.15. The numerical model represents the regulator in its current condition using the deteriorated material properties. Nonlinear analysis is performed to assess the structural safety of the regulator under the current applied dead, live loads, and the worse expected loading condition; also, to determine the structural efficiency, safety margin and strengthening requirements. The numerical results and the proposed strengthening for the regulator will be presented and discussed.



**Keywords:** masonry, vault, hydraulic structure, assessment, finite elements, nonlinear analysis.

## 1. INTRODUCTION

Regulators are hydraulic structures that are constructed at the beginning of an irrigation channel and along its length in order to control water discharge from the upstream to the downstream of the canal. In Egypt, hundreds of regulators have been constructed since 1860 on the River Nile and its branches. The old hydraulic structures constructed of stone or brick masonry have been exposed to severe conditions and excessive loading for long years, reaching 100 to 150 years. This has led in many cases to material deterioration, cracking and observed damage to the main structural elements, which threatens the serviceability and safety of these economically important structures. Research is needed to investigate the structural condition of these structures and accurately evaluate their behavior under the applied and expected loading conditions.

Several studies addressed this important topic. D'Altri et al. [1] presented a numerical procedure for the force-displacement description of out-of plane collapse in masonry structures. Limit-analysis based solutions were considered to investigate collapse mechanisms in masonry structures. Several meaningful structural examples show the effectiveness of the numerical procedure proposed.

Degli Abbati et al. [2] perform a numerical modeling using nonlinear static analyses for the seismic evaluation of masonry structures. The proposed study contain modal analysis on the 3D finite element model for the masonry structure to define the modes of vibrations that contains dynamic response of each unit and their modal shapes. The study results are promising and can be extended to study complex historic structures.

An example of a typical old regulator in Egypt is considered in this study; Bahr-Mowees Regulator constructed in 1888 and located on the right bank of El-Tawfiki Rayah at km 35.00. Numerical modeling is made using finite elements and nonlinear analysis is performed using commercial software ANSYS v.15 [3]. The finite element model and nonlinear analysis parameters are described. The numerical results are presented in terms of deformations and stresses.

Pulatsu et al. [4] presented 3D simulation for masonry arch bridge with different failure mechanisms. Discrete element method (DEM), was used to evaluate the effect of essential structural elements, such as the arch barrel, spandrel wall and back-fill material on many masonry arch structures. The ultimate Load, and different failure mechanisms were evaluated using parametric studies on the mechanical properties of backfilling material. The results indicate that soil mechanical properties have noticed effect on the structural behavior and ultimate load of the studied masonry arch bridges.

Cavicchi and Gambarotta [5] presented a two dimensional model to evaluate the ultimate load of masonry arch bridges. The proposed numerical model are shown in two examples. The first example concerns a real bridge tested up to failure and shows that the model can provide good cagreemnt with the experimental results. The second model for multi-span bridge shows the ability of the model describe the complex interaction between piers, arches and fill at failure.

Milani and Lourenço [6] perform 3D finite element modeling with static nonlinear behavior for masonry bridges. Two full scale masonry bridges were analyzed. A skew single span structure experimentally tested till collapse and a straight multi span bridge with five circular arches was loaded with an eccentric load at the Bolton Institute, UK. Both two dimensional and three dimensional limit analyses were performed to get the actual capabilities of the 3D approach to reproduce the ultimate loads and deformed shapes at collapse and, also to investigate limitations of 2D assumptions when transversal effects resulted by arch geometry and load eccentricity are not considered.



Castellazzi et al. [7] presented a procedure applied for the structural health assessment of the railway masonry arch bridge crossing the Reno River in Bologna (Italy. Accurate static and dynamic load tests have been performed on some arches whereas simplified dynamic tests have been repeated on all the spans of the bridge in order to verify the homogeneity of their structural behavior. The tuned finite element model has been used for the evaluation of the structural health of the bridge both in its actual state and in the hypothesis of a structural strengthening intervention.

Cakir and Seker [8] studied several masonry bridges and focused on Low Bridge, an example of renovated masonry bridges in Turkey, to assess the structural behavior of the masonry bridge and investigate the integrity of the renovated components. The mechanical properties of the bridge material were first evaluated with experimental tests, then static modal and nonlinear time history analyses were carried by finite element methods to investigate the structural behavior of the current form of the bridge.

Reccia et al. [9] presented different procedures to evaluate nonlinear behavior of masonry arch bridges. The Venice trans-lagoon masonry arch bridge was analyzed using many three-dimensional finite element modeling. The bridge was loaded with the passengers working loads and both single and double track standard loads till collapse. Results of the nonlinear modeling were compared with limit analysis predictions of failure loads and failure mechanisms.

Atamturktur and Laman [10] presented a study of assessment of historic masonry monuments and focused on complex vaulted masonry such as masonry arch bridges, due to its irregular geometry,

complex material behavior and complicated boundary conditions. Studies on simpler forms of masonry structures, such as masonry arch bridges or masonry towers, were also discussed since they lay the groundwork for studies on more complex structures. As a result of this review, it is apparent that the ever-increasing popularity of FE model calibration will result in the routine application of model calibration to a diverse group of masonry structures.

Cavicchi and Gambarotta [11] present a 2D model to evaluate a masonry bridges takes into account the strengthening effects due to arch–fill interaction observed in experimental tests. Upper bounds on the collapse load and the corresponding mechanism were obtained by means of a finite element application of the Kinematic Theorem of Limit Analysis.

## 2. STRUCTURE DESCRIPTION

Bahr-Mowees Regulator is a Head Regulator on El-Tawfiki Rayah at km 35.00 on the right bank, it was constructed in 1888. The regulator has 7 gates with openings of 3.00 m each width separated by masonry piers, the piers support a masonry roadway arch bridge. All the supporting systems of piers, abutments, and wing walls are constructed of clay bricks with masonry built over a concrete apron raft founded on the canal bed. The upstream and downstream views of the regulator are shown in Fig. 1 and 2, together with longitudinal and cross sections. And regulator dimensions are listed in table 1,2.



(b) Upstream view (c) Downstream view

Fig. 1. Bahr-Mowees regulator

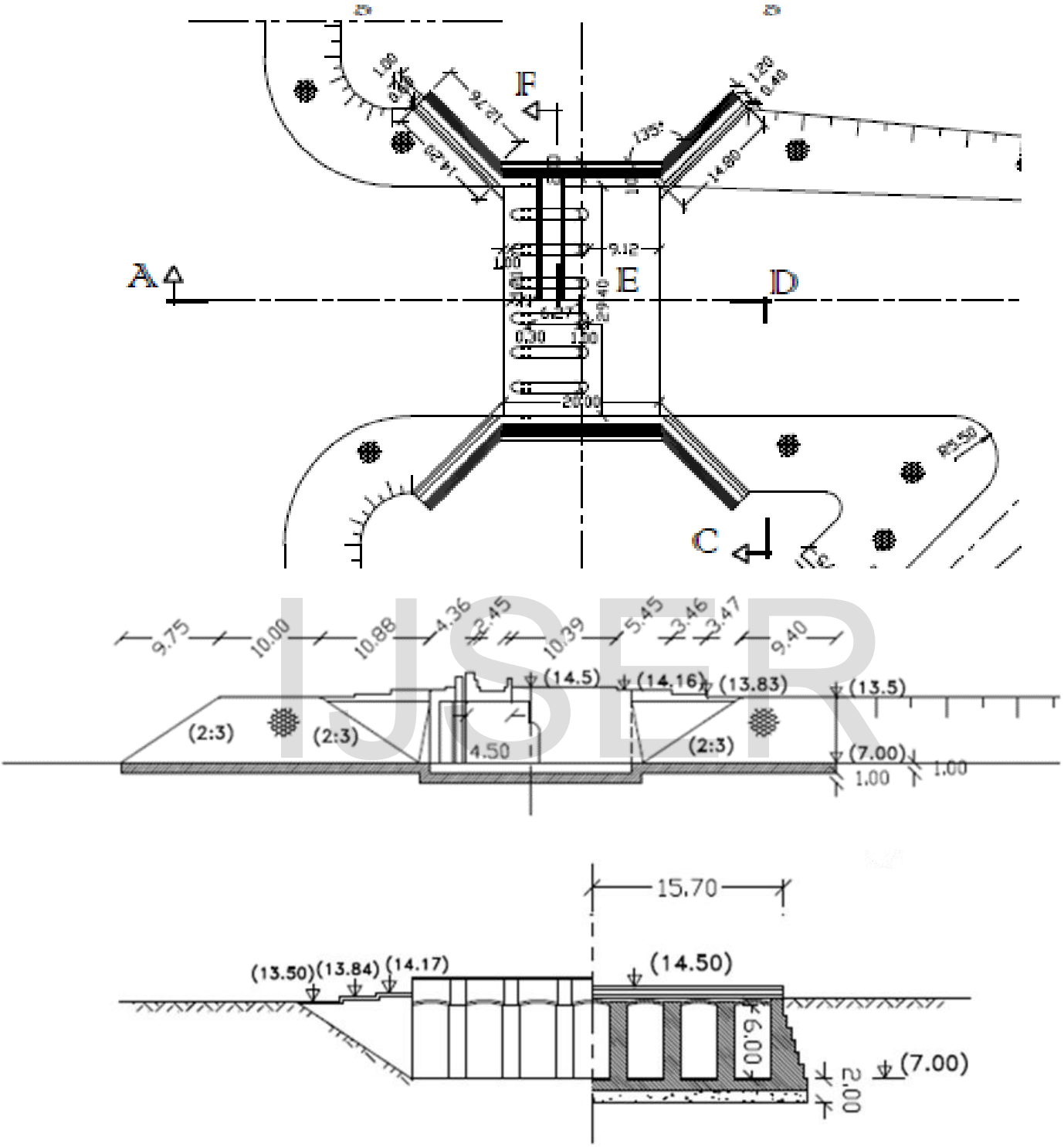


Fig. 2. Plan, longitudinal and cross sections of the regulator

Table 1: General Dimensions of BahrMowees Regulator

| Item | Dimension or levels |
|---|---|
| Total number of gate openings | 7 |
| Gate opening | 3.00 m |
| Pier height | 6.00 m |
| Roadway level | (14.50) |
| Pier<br>• Length<br>• Thickness<br>• Top elevation<br>• Bottom elevation | 9.88 m<br>1.40 m<br>(13.00 m)<br>(7.00m) |



Table 2: Hydraulic Data of BahrMowees Regulator

| Item | Level |
|---|---|
| Maximum upstream water level | 12.80 |
| Minimum downstream water level | 9.70 |
| Maximum allowed head difference | 2.00 m |

## 3. SITE INVESTIGATION AND MATERIAL TESTS

Site investigation was carried out for Bahrmowees head regulator within a national project performed for assessment of Egypt's major hydraulic structures [12]. The investigation can be presented in two parts.

### 3.1 GEOTECHNICAL INVESTIGATIONS

Nine boreholes were mechanically advanced down to depth of 18.75 m below ground level. The layout of the boreholes is shown in Fig. 3.a. The boreholes were drilled using a rotary-drilling machine in order to obtain samples for classification, laboratory testing and groundwater information, and geotechnical longitudinal profile along the site based on the results of this investigation the samples of boreholes shown in Fig. 3.b. The samples extracted from boreholes are shown in Fig. 4.

### 3.2 MATERIAL TESTS ON CORE SAMPLES

This section includes the results of core tests that were performed on masonry and concrete samples extracted from abutments and piers at Bahr mowees head regulator. The target is to evaluate the compressive strength of the masonry and concrete. A total of 17 core samples were extracted. Two core samples were kept without testing for the purpose of further determination of the elastic modulus, therefore 15 core specimens were tested under compression, compression tests procedure for some samples are shown in Fig. 5. Table 3 shows material properties of the regulator elements which are resulted from the tests made on the cores extracted from the regulator elements.

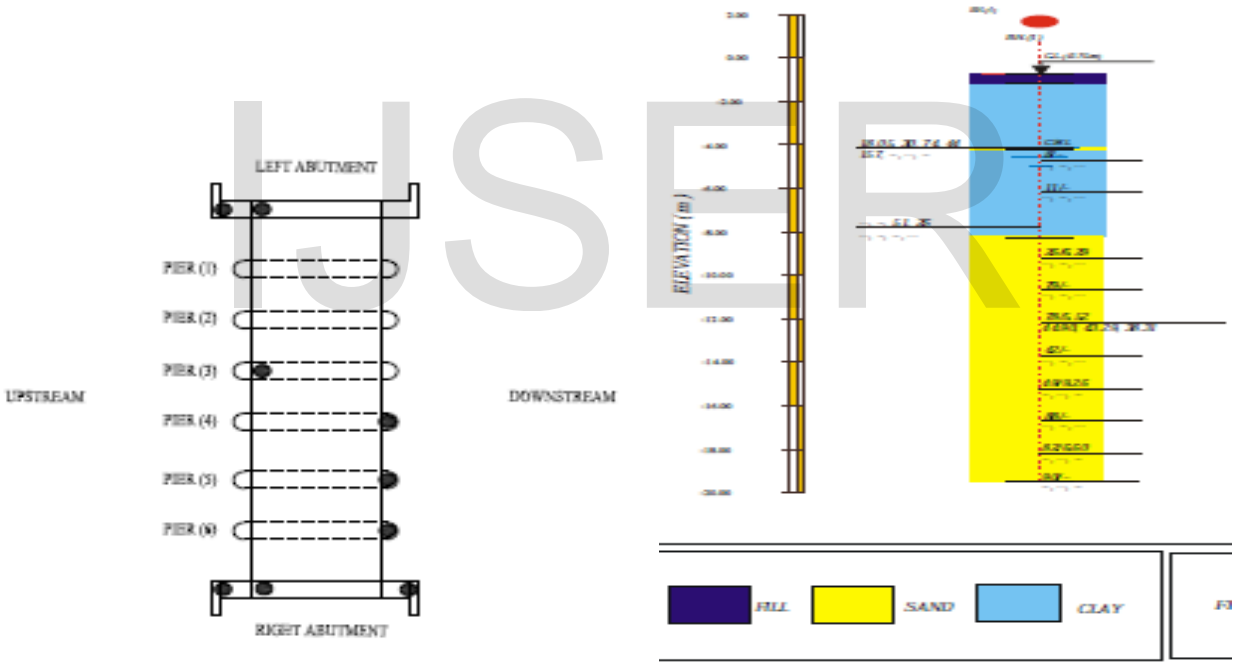


(a) (b)

Fig. 3. a) Layout of the boreholes, b) Simplified longitudinal geotechnical section [12]

Fig. 4 Samples extracted from boreholes [12]

Fig. 5 Compression testing in laboratory of core samples [12]

TABLE 3. MATERIAL PROPERTIES DETERMINED FROM TESTS

| Material | Unit weight ($\gamma$) t/m$^3$ | Max. comp. (kg/cm$^2$) | Min. comp. (kg/cm$^2$) | Avg. comp. (kg/cm$^2$) | Comp. (ACI) (kg/cm$^2$) | Tension (kg/cm$^2$) (assumed) |
|---|---|---|---|---|---|---|
| Red Brick | 1.612 | 41.4 | 16.4 | 28.9 | 43 | 4.3 |
| Stone | 2.06 | 249.2 | 44.2 | 146.7 | 44.2 | 19.75 |

## 4. NUMERICAL MODELING AND NONLINEAR ANALYSIS

### 4.1 MODELING AND NONLINEAR ANALYSIS APPROACH

Different modeling strategies may be followed to represent the heterogeneous and anisotropic nature of masonry construction by finite elements, depending on the level of accuracy and the simplicity desired. These strategies are described as follows [13-15].

(a) Detailed micro-modeling: the mortar and masonry units are modeled as independent elements with independent mechanical properties, interface element between mortar and masonry shall be assigned to simulate the bond between the two elements. This kind of modeling is very complex and valid for research or small models for localized areas.

(b) Simplified micro-modeling: in this type of modeling strategies masonry units are represented by individual elements where the bonding between the units (mortar) are modeled using interface elements [16].

(c) Macro-modeling (homogenization theory): the masonry units, mortar and mortar-unit interface are smeared out in a homogenous continuum material. Macro models are more applicable when the structure has large dimensions and stresses are uniformly distributed along the macro-length [17, 18]

### 4.2 FINITE ELEMENT MESH

In this research work, modeling and analysis of the regulator is performed through macro-modeling, where masonry consisting of brick units and mortar is considered a homogenous continuum for which the macro behavior is simulated through selection of specific material properties. The commercial computer software ANSYS v.15 [3] is used for finite element discretization and nonlinear analysis. A three-dimensional finite element model was made for the whole regulator structure. The masonry components (arches, abutment, wing walls and piers) are represented by solid elements; the finite element mesh is shown in Fig 6.

### 4.3 MATERIAL PROPERTIES

Multilinear isotropic hardening material is used to simulate the masonry composite (brick and mortar) and the mortar layers, described by a multilinear stress-strain curve. Laboratory tests were made on cores extracted from the regulator elements, the determined material properties are listed in Table 3. The material properties of masonry adopted in the analysis are as follows:

- Masonry compressive strength ( f'm ) = 4250 kPa Modulus of Elasticity ( Em ) = 595000 kPa
- Weight density = 18 kN/m3
- Major Poisson's ratio = 0.15
- Tensile strength assumed to be 0.1 f'm = 425 kPa.
-

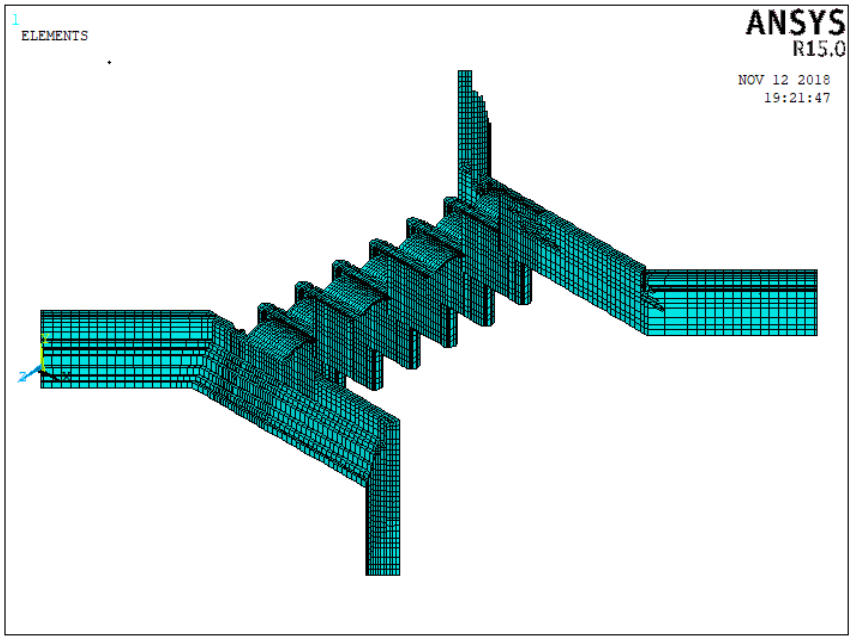


Fig 6. Three-dimensional finite element mesh

### 4.4 LOADS AND LOAD CASES

The loads acting on the regulator structure were calculated, listed as follows.

1. Dead load: consists of the own weight of the masonry and earth fill material.
2. Live load: vehicles and pedestrian loads on the roadway and bridge.
3. Water static pressure on piers, abutment, and raft, calculated for the upstream and downstream from the equation:

   $Pw = \gamma w * h$ where: $\gamma w = 10\ kN/m^3$ and h = depth of water
4. Earth pressure: static earth pressure on abutment and wing walls, calculated as

   $P = Ks * hs * ka$ Where: $\gamma s$ = soil density, hs= depth of soil column, and

   $ka = (1 - \sin\phi) / (1 + \sin\phi)$.
5. Surcharge: Surcharge of about 1.0 $t/m^2$ distributed on soil behind the wing wall due to effect of traffic was taken into consideration for earth pressure calculation

The regulators structures are usually subjected to different load cases during its life time such as construction, operation, Taharek cases and deterioration for this regulator as follows.

**Case A**: Construction case in which the regulator is subjected to its own weight, earth pressure and surcharge.

**Case B**: Operation: maximum upstream water level (11.70) and downstream water level (9.70).

**Case C**: Taharek: maximum upstream water level (11.70) and downstream water level (0.00).

**Case D**: Deterioration: material properties are assumed to be 50% of the mechanical properties of the existing structure.

### 4.5 NONLINEAR ANALYSIS PARAMETERS

The nonlinear analysis parameters adopted are as follows:

- Shear coefficient along opening cracks (ShrCf-pO) = 0.2, the coefficient present the amount of shear force can transfer along open crack.
- Shear coefficient along closed cracks (ShCf-Cl) = 0.8, the coefficient present the amount of shear force can transfer along closed crack
- Tension limit, cracking limit (UnTensSt) = 425 kPa
- Compression limit, crushing limit (UnCompSt) = 4250 kPa

## 5. NUMERICAL RESULTS

The results obtained from the nonlinear analysis regarding deformed shape in x- y- and z-direction and stresses in x- y- and z- directions due to the studied load cases are shown in Figs 7 to 13.

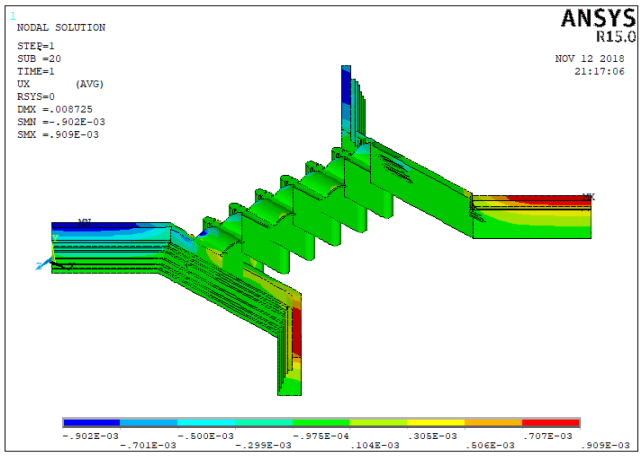


Case (a)

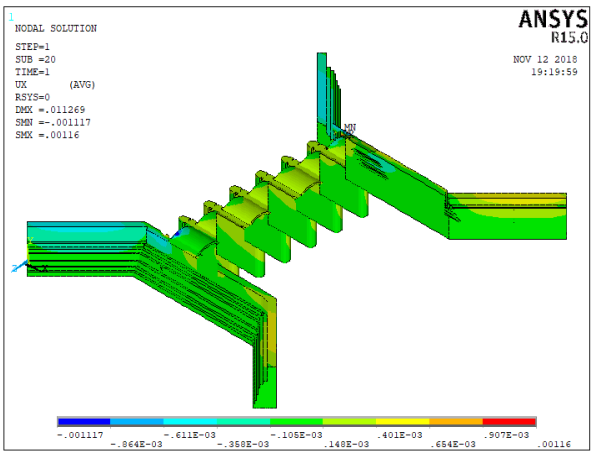


Case (b)

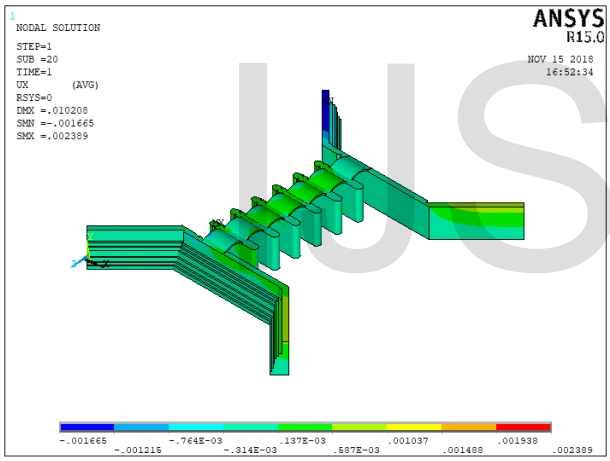


Case (c)

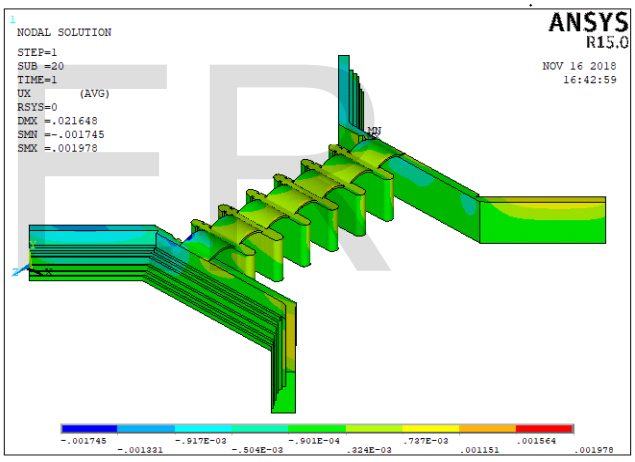


Case (d)

Fig. 7 Deformed shape in x-direction (regulator longitudinal axis) (displacement in m)

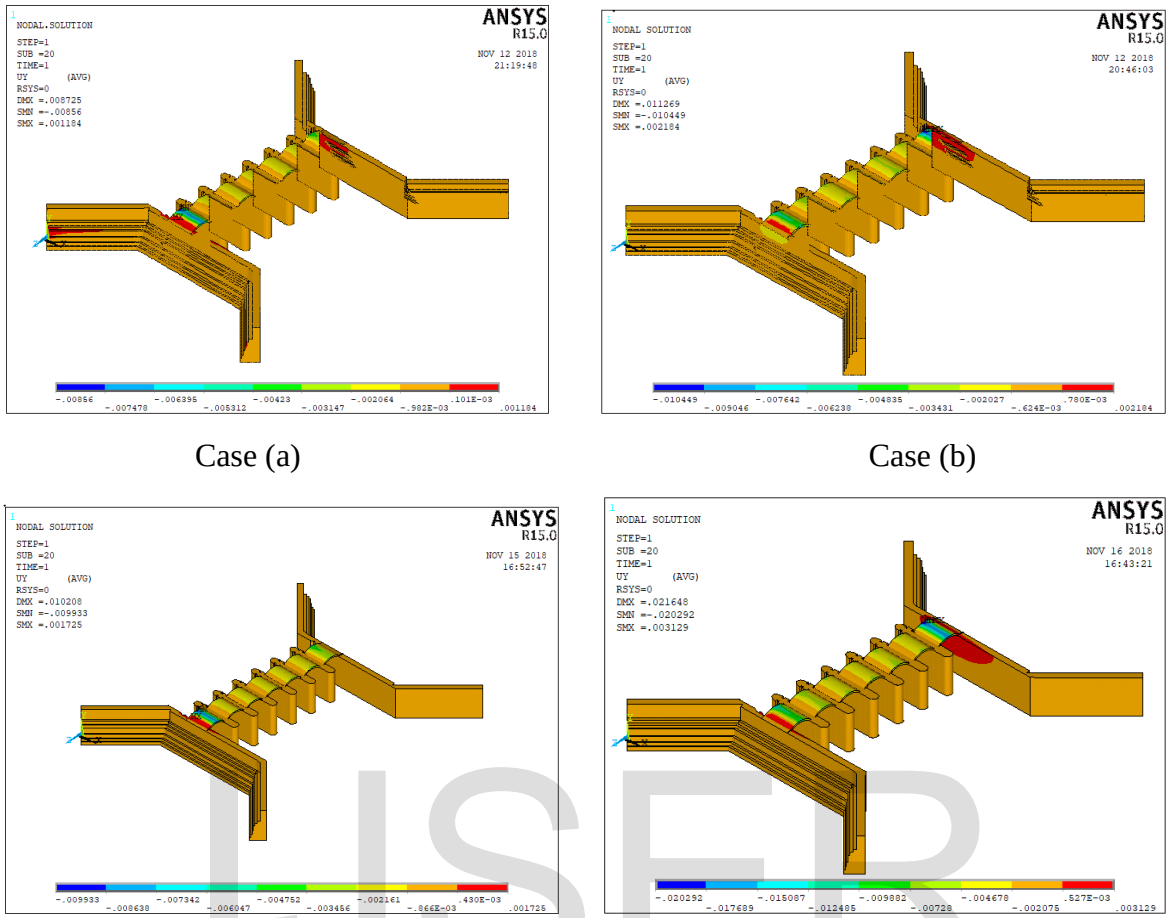


Fig. 8. Deformed shape in y-direction (transverse direction) (displacement in m)

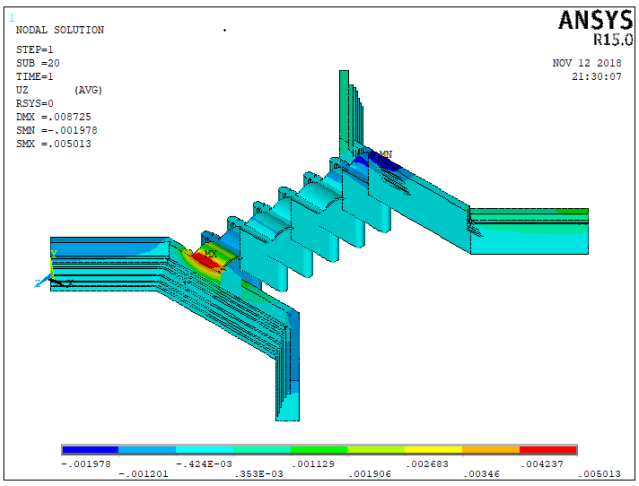


Case (a)

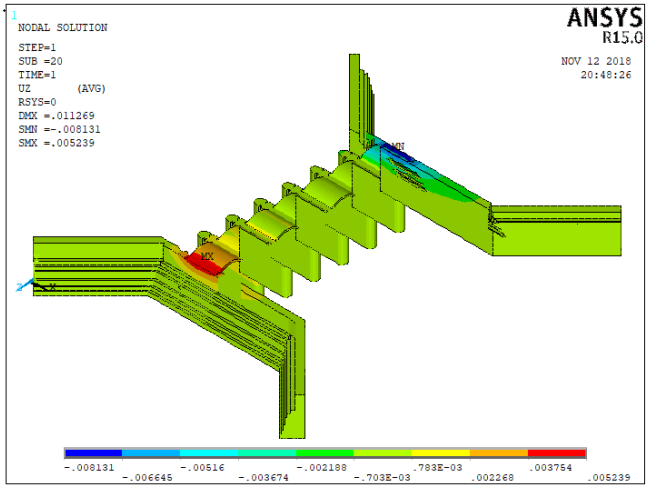


Case (b)

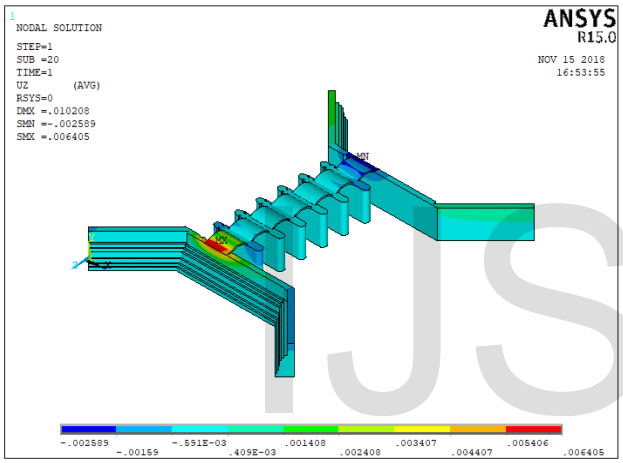


Case (c)

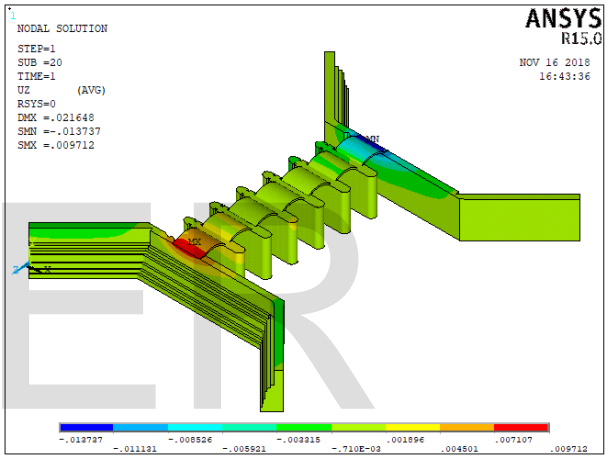


Case (d)

Fig. 9. Deformed shape in z-direction (vertical direction) (displacement in m)

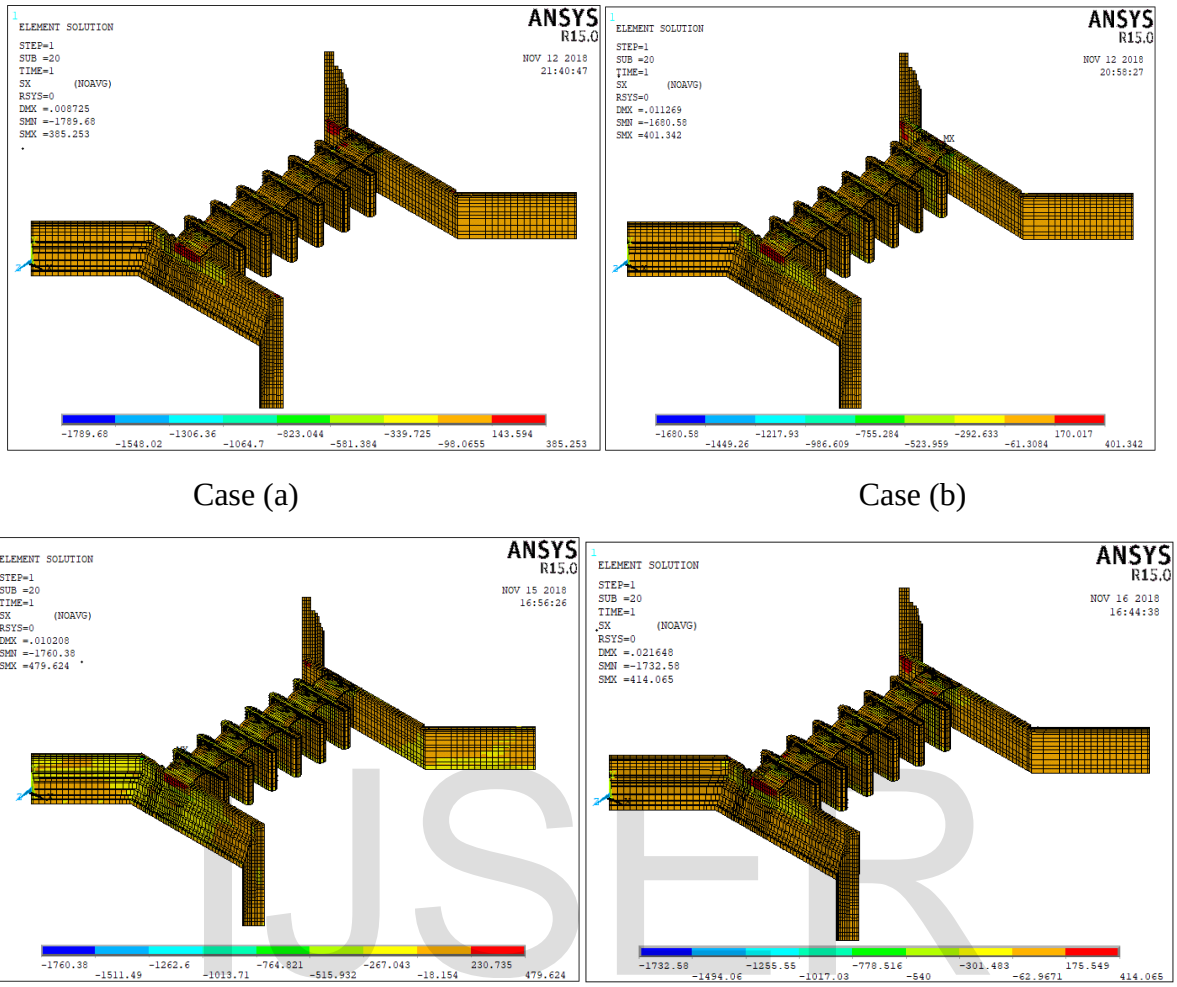


Case (a) Case (b)

Case (c) Case (d)

Fig. 10. Stresses in x-direction, in kPa.

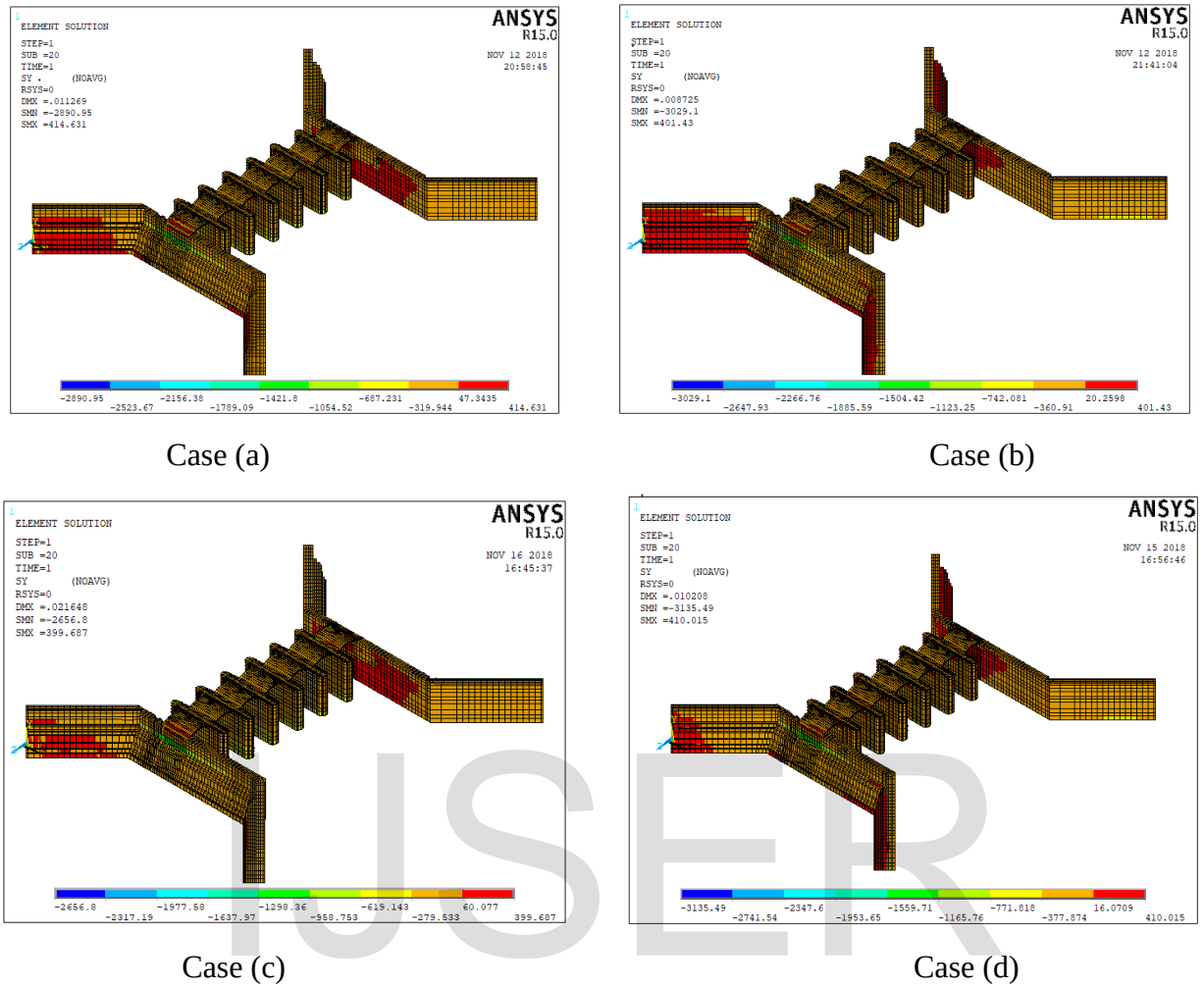


Fig. 11. Stresses in y- direction, in kPa.

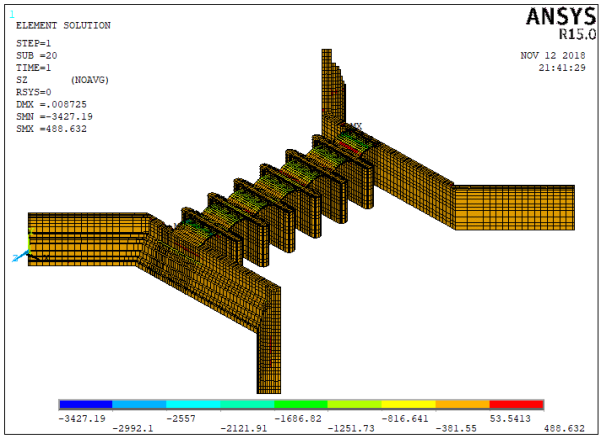


Case (a )

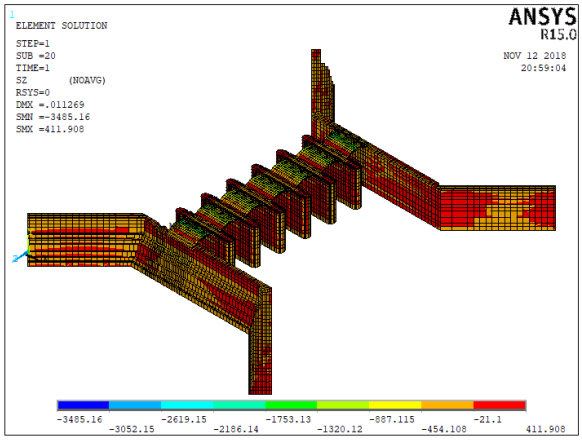


Case (b)

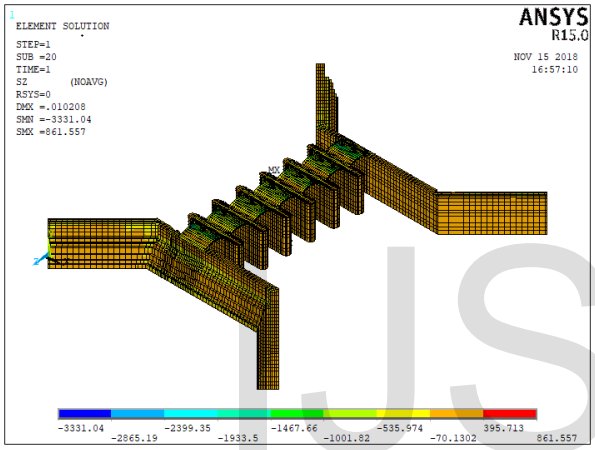


Case (c)

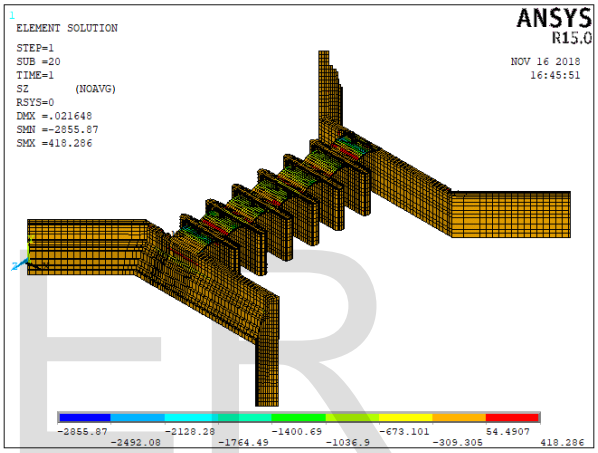


Case (d)

Fig. 12. Stresses in z-direction, in kPa.

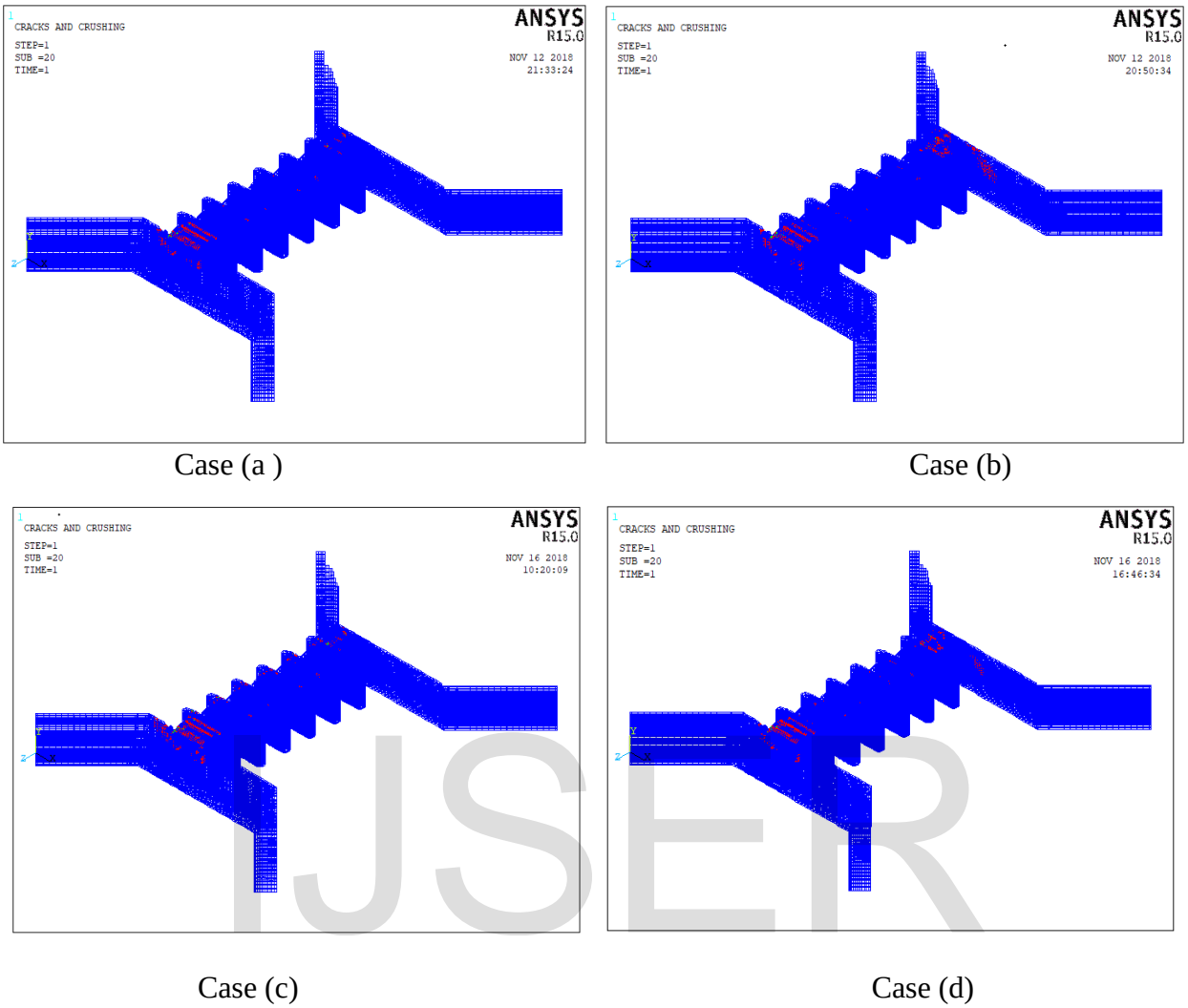


Case (a ) Case (b)

Case (c) Case (d)

Fig. 13. Crack pattern for different load casese.

## 6. DISCUSSION OF RESULTS

For construction case, the deformation in y direction of wing wall is 1.18 mm and 8.56 mm, because of effect of back fill and earth pressure as shown in Fig. 8(a) and fig 15, stress is maximum value in y direction of wing wall, tension 401.34 kPa and compression -3029.1 kPa as shown in Fig.11(a), also crack pattern illustration is shown in fig 16.

In the operation case, the deformation maximum existing in wing wall in y direction are 1 mm and 6 mm as shown in Fig. 8(b), stresses in y direction are tension 390 kPa and compression -2890.95 kPa as in Fig. 11(b).

In Taharek case of loading and when the gate of the regulator is closed a maximum water level applied on the gates on the upstream side and there is no water at the downstream. that cause deformation in y direction 1.7 mm and -9.9 mm as shown in Fig. 8(c), stresses in y direction of wing wall are tension 410 kPa and compression 3135 kPa Fig. 11(c).

In the Deterioration case, the deformation increased on wind wall downstream in y direction 3 mm and -20.2 mm, shown in Fig. 8(d). Stresses increased in wing wall in direction of y on wing wall tension 399.6 kPa and compression 2656 kPa as shown in Fig. 11(d).

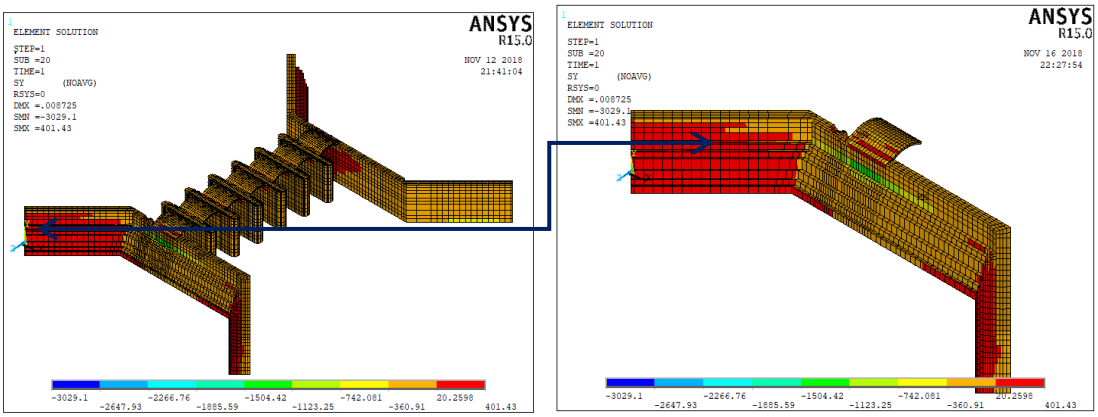


Fig. 14 Stresses in y direction of Bahrmowees Regulator - Construction case

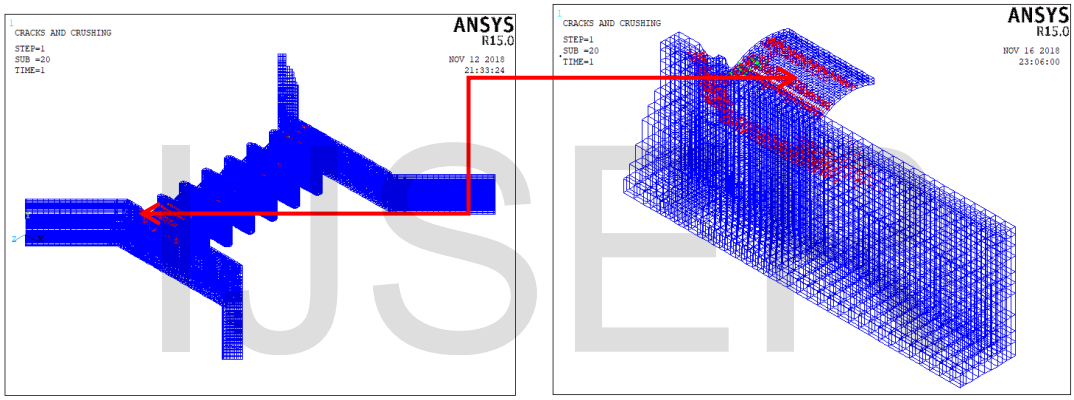




Fig. 15 Cracking pattern of Bahrmowees Regulator - construction case

## 7. STRENGTHENING OF THE REGULATOR USING STEEL RODS

In light of the previous results it have been concluded that the wing wall of the regulator suffer from extra stresses specially in construction and Taharek case of loading, the Numerical modeling and structural analysis were made for Bahrmowees regulator with strengthening. The mechanical properties of material were reduced to 50% of its efficiency, under this case of loading some cracks occurred in the wing wall especially in the upstream, stresses in y direction are shown in Fig. 14. And crack pattern shown in fig 15.

A steel tie rods are used to reinforce the wing wall vertically as shown in Fig. 16. For comparison, the cracks are shown in Fig. 17. The numerical results indicate that the maximum occurring stresses were decreased from 598 kPa to 294 kPa after using the tie rod. This means that the wing wall restored its efficiency and the cracks decreased.

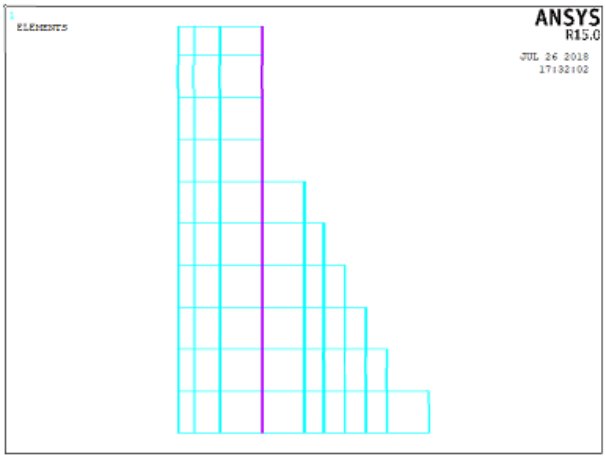


Fig. 16 Suggested reinforcement for the wing wall of Bahr mowees regulator

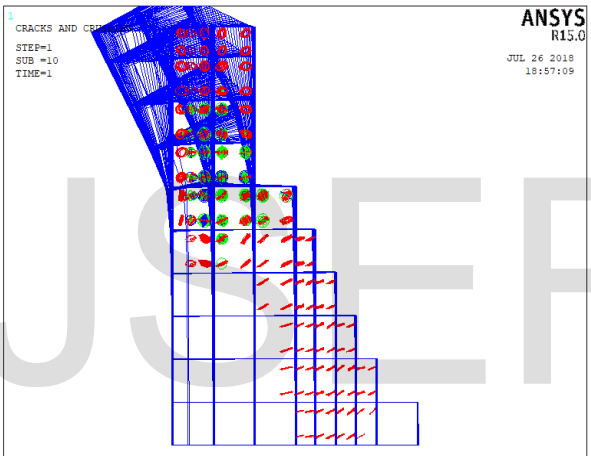


a) unstrengthened

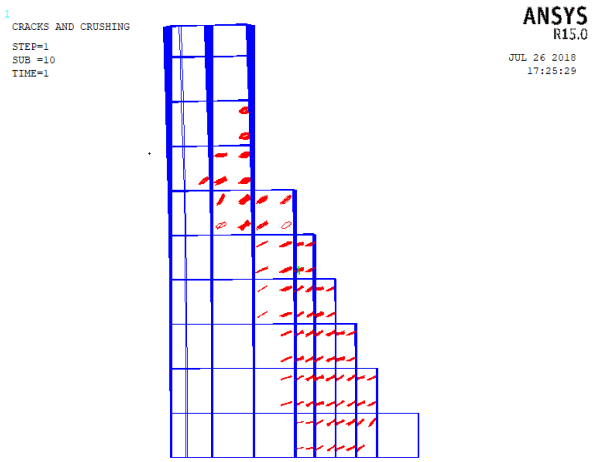


b) strengthened

Fig. 17 Cracks in Bahr Mowees regulator wing wall before and after strengthening

## 8. CONCLUSION

In this paper, a three-dimensional finite element model was made for an old masonry regulator using the macro-modeling approach; the exact geometry and current condition are represented including characterization of material properties. Numerical modeling and nonlinear analysis were made using commercial software ANSYS v.15. The structural behavior was studied under four different loading conditions. Strengthening was proposed for the wing wall using steel reinforcement bars.

- The arch was exposed to maximum tension value at construction load casing because the effect of the vertical loads (dead and live loads), in the operation case due to the existing of water pressure against the lateral loads (earth pressure) tension increased in the bottom of arch because of the difference between lateral loads and water pressure, for the deterioration case tension and compression value are within range of the allowable 425 kPa for tension and 4250 kPa for compression.
- Wing walls upstream and downstream are exposed to moment due to lateral earth pressure with maximum value in construction and reduced in operation with the exist of water pressure against lateral loads, in Taharek load case downstream wing wall exposed to tension value bigger than upstream wing wall due to maximum water level in upstream and zero water in downstream, as for the deterioration load case it observe that tension value upstream wing wall increased to 650 kPa which explain the cracks occurred in wing wall because it is more than the allowable tension value 425 kPa.
- The gate exposed to tension which increased gradually to 67 kPa in taharek load case because of the maximum water pressure on it, and increased in deterioration load case tension is 85.9 kPa but still in the allowable tension zone.
- Piers exposed to compression equal -822 kPa and tension equal 198 kPa due to the vertical load ( dead and live ), but still in the allowable stress zone.
- Over all the regulator is safe under existed loads except notice some cracks in wing wall under construction and deterioration load case.
- The strengthening of the wing wall in accordance with the previous results have been performed using steel rods, and the numerical results indicate that the maximum occurring stresses were decreased and wing wall deformation is also decreased, and the wing wall restored its efficiency and also the cracks decreased.

## Compliance with Ethical Standards:

The authors declare that they have no conflict of interest.

## 9. REFERENCES

[1] D'Altri, A. M., de Miranda, S., Milani, G. and Castellazzi, G. (2020). A numerical procedure for the force-displacement description of out-of-plane collapse mechanisms in masonry structures. Computers & Structures, 233, 106234.

[2] Degli Abbati, S., D'Altri, A. M., Ottonelli, D., Castellazzi, G., Cattari, S., de Miranda, S. and Lagomarsino, S. (2018). Seismic assessment of interacting structural units in complex historic masonry constructions by nonlinear static analyses. Computers & Structures.
[3] ANSYS v.15, ANSYS® Nonlinear Analysis Computer Program, Release 15.0, Theory Reference Manual, ANSYS Inc., Canonsburg, PA, USA, 2015.

[4] Pulatsu B., Erdogmus E. and Lourenco P.B. Simulation of Masonry Arch Bridges Using 3D Discrete Element Modeling, Structural Analysis of Historical Constructions , ISBN 978-3-319-99441-3, Vol. 18, Pg. 871, September 2018.

[5] Cavicchi A. and Gambarotta L. Two-Dimensional Finite Element Upper Bound Limit Analysis of Masonry Bridges", Science Direct, October 2006.

[6] Milani G. and Lourenço P.B., 3D Non-Linear Behavior of Masonry Arch Bridges, Elsevier, Computers and Structures, August 2012.

[7] Castellazzi G., De Miranda S. and Mazzotti C., Finite Element Modelling Tuned on Experimental Testing for the Structural Health Assessment of an Ancient Masonry Arch Bridge, Hindawi Publishing Corporation Mathematical Problems in Engineering, Vol. 2012, Paper ID 495019, August 2012.

[8] Cakir F. and Seker B. Structural Performance of Renovated Masonry Low Bridge in Amasya, Turkey, Earthquakes and Structures, Vol. 8, No. 6 (2015) ISBN 1387-1406, November 2014.

[9] Reccia E., Milani G., Cecch A. and Tralli A. "Full 3D Homogenization Approach to Investigate the Behavior of Masonry Arch Bridges: The Venice Trans-Lagoon Railway Bridge", Construction and Building Materials, ISN 66-567–586, June 2014.

[10] Atamturktur S. and Jeffrey A., "Finite Element Model Correlation and Calibration of Historic Masonry Monuments", The Structural Design of Tall and Special Buildings, April 2010.

[11] Cavicchi A. and Gambarotta L., "Collapse Analysis of Masonry Bridges Taking into account Arch–Fill Interaction", Engineering Structures, ISSN 27/605–615 October 2006.

[12] Reservoirs and Grand Barrages Sector (RGBS), Geotechnical and Structural Report, Bahrmowees Head Regulator, December 2014.

[13] Lourenco P.B. Computations on historic Masonry structures, Prog. Struct. Mat. Eng. 4 (3) (2002) 301–319.
[14] P. Roca, M. Cervera, G. Gariup, Pelà L. Structural analysis of masonry historical constructions, classical and advanced approaches, Arch. Comput. Meth. Eng. 17(3) (2010) 299–325.
[15] Giordano A., Mele E. and de Luca A. (2002). Modelling of Historical Masonry Structures: Comparison of Different Approaches Through a Case Study", Engineering Structures, Vol.24, No. 8, pp. 1057–1069.
[16] Giambanco, G., Rizzo, S. and Spallino, R. (2001), "Numerical Analysis of Masonry Structures via Interface Models", Computer Methods in Applied Mechanical Engineering, Vol. 190, No. 49–50, 2001, pp. 6493–6511.
[17] Chen, S.Y., Moon, F.L. and Yi, T. (2008), "A Macro-element for the Nonlinear Analysis of In-plane Unreinforced Masonry Piers", Engineering Structures, Elsevier, Vol.30, No.8, 2008, pp. 2242–2252.

[18] Milani, G., and Lourenco, P.B. (2012), "A Simple Homogenized Model for the Nonlinear Analysis of FRP-Strengthened Masonry Structures". Proceedings of the Eleventh International Conference on Computational Structures Technology, Civil-Comp Press, Stirlingshire, Scotland, 2012.